Electronic Step Down (220/110 V) Transformer Using a New Quantum Series Resonant Converter

Dong-Young Huh and Gyu-Hyeong Cho

Abstract—**A new Quantum Series Resonant Converter (QSRC) topology for pure sinewave 60 Hz ac chopper is proposed. It has three bidirectional switches and operates at high switching frequency with low switching loss. Bidirectional power flow is possible and the switches can operate at either zero current switching (ZCS) mode or zero voltage switching (ZVS) mode by slight modification. The QSRC is thought to be suitable for such a system with fixed voltage conversion ratio. The proposed converter is applied to an electronic 220/110 V transformer. The detailed analyses and the experimental results for 1 kVA are presented.**

I. Introduction

THE step up of the line voltage from 110 to 220 V ac reduces the loss in the power transmission line by one fourth, or transmits four times more power with the existing line for the same loss. Many electric equipments, however, still use 110 V ac and step down transformers are needed. Iron cored transformer has the features of low cost, good efficiency and high reliability. On the other hand, the conventional transformer is heavy and bulky and it has substantial amount of no load loss. No load loss is very important because the transformer is usually connected 24 hours a day and consumes energy. Especially if the operation duty of the equipment is low such as microwave oven, washer, refregerator, etc., the total efficiency of the transformer becomes poor even if the full load efficiency is very good. If the no load loss is counted nation wide, it becomes tremendous amount.

On the other hand, electronic transformer can be made with negligible no load loss. Thus it has considerable advantage over the conventional iron cored transformer in such a kind of applications where the operation duty is low even if the full load efficiency is somewhat lower. Besides the weight and size of the electronic transformer can be significantly reduced by using an ac chopper with high switching frequency.

Recently many soft switching converters have been reported for their merits such as high efficiency, high power density and high performance, etc. [1]–[6]. Among them the quantum converter has all of the merits of the soft switching converters and can easily be modeled to a conventional PWM-like converter [7],[8]. The voltage conversion ratio, however, is quantized in the quantum converter and it is somewhat difficult to control the output voltage with good precision between the quantized levels. But it is suitable for such a system with fixed voltage conversion ratio such as the electronic transformer.

In this paper, an analytical method of deriving the voltage conversion ratio of the quantum converter is described and applied to a new quantum series resonant converter (QSRC). A zero-voltage-switching QSRC is also proposed. The proposed ZCS QSRC and ZVS QSRC are applied to the ac chopper (electronic transformer) which has pure sinewave 60 Hz input and out and the design equations are derived.

Manusript received December 20, 1991; revised February 26, 1993. This work was supported by the Korea Electric Power Cooperation.

The authors are with the Department of Electrical Engineering, Korea Advanced Institute of Science and Technology, Yusong-gu Taejon 305-701 Korea.

IEEE Log Number 9211697.

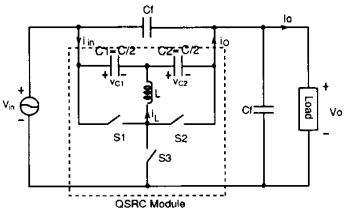

(a)

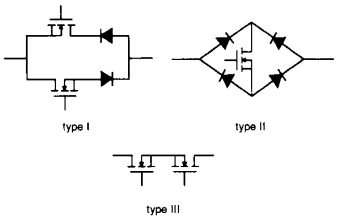

(b)

Fig. 1. (a) The proposed power circuit of the ac chopper. (b) Bi-directional switches.

II. Basic Structure of AC Chopper

Fig. 1(a) shows the proposed power circuit of ac chopper. The part inside the dotted line shows the proposed QSRC module. QSRC module has two resonant capacitors (C_1 and C_2), one resonant inductor (L) and three switches (S_1, S_2, and S_3). Symmetrical L-C structure is to reduce the current ripple. All of the switches are bi-directional as illustrated in Fig. 1(b) for four quadrant operation. The switches are always switched on and off very near to zero resonant inductor current.

Since the line frequency is quite lower than the switching frequency, the output voltage has the same waveform and frequency as the input voltage by controlling the three switches with a fixed switching procedure. The ratio of the input and output voltage can be set to any desired value as the conventional iron cored step-down transformer. To get 110

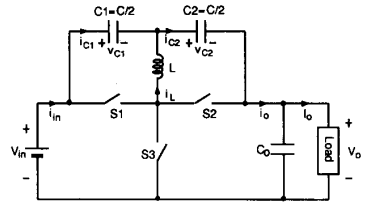

Fig. 2. QSRC module with dc input voltage

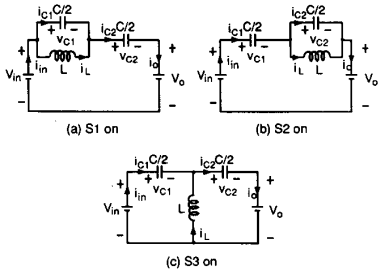

Fig. 3. Equivalent circuits for each switch condition.

from 220 V ac of line voltage, the switching sequence is given by $S1$-$S2$-$S3$-$S2$. In the case of output short circuit, however, the switching sequence is changed to $S2$-$S3$-$S2$-$S3$ for protection. Two C_fs' are both for the input and the output filter capacitors and splitted in this way so that the voltage of the output is one half of the input at no load condition without operating the switches.

III. DC Operation of QSRC Module

A. Analysis of The Basic Operation

For simplicity, Fig. 2 shows the QSRC module for dc supply case instead of ac. At any time, only one switch is in conduction. Switching operation occurs at the instant of every zero inductor current and the ON duration of each switch is the half resonant period of L and C. The resonant tank circuit parameters are

$$z_r = \sqrt{\frac{L}{C}} \tag{1.1}$$

$$\omega_r = \frac{1}{\sqrt{LC}} \tag{1.2}$$

$$T_r = 2\pi\sqrt{LC} \tag{1.3}$$

By low ripple approximation [9], the output voltage V_o can be regarded as constant for a fixed switching pattern. The sum of the two capacitor voltages, $v_{c1} + v_{c2}$, is always constant. Thus we can write

$$\frac{dv_{c1}}{dt} + \frac{dv_{c2}}{dt} = 0. \tag{2.1}$$

For the case $C_1 = C_2 = C/2$,

$$i_{c1} = -i_{c2} = -\frac{1}{2}i_L. \tag{2.2}$$

Therefore the inductor current flows through C_1 and C_2 with the same magnitude but in opposite direction. Circuit equations can be given as follows for each switch conduction state by assuming all of the switches, inductors and capacitors ideal.

S1 conduction state Fig. 3(a) shows the equivalent circuit when $S1$ is conducting. The initial conditions are assumed as

$$i_L(0) = 0, \quad v_{c1}(0) = V_{11}, \quad v_{c2}(0) = V_{21}. \tag{3.1}$$

Then the inductor current and the capacitor voltages are given by

$$i_L(t) = \frac{V_{11}}{z_r}\sin\omega_r t = \frac{(V_{in} - V_o - V_{21})}{z_r}\sin\omega_r t \tag{3.2}$$

$$v_{c1}(t) = V_{11}\cos\omega_r t = (V_{in} - V_o - V_{21})\cos\omega_r t \tag{3.3}$$

$$v_{c2}(t) = (V_{in} - V_o - V_{21})(1 - \cos\omega_r t) + V_{21}. \tag{3.4}$$

The input and output currents are

$$i_{in}(t) = i_o(t) = \frac{1}{2}i_L(t) \quad \text{where} \quad 0 \le t \le \frac{T_r}{2}. \tag{3.5}$$

S2 conduction state Fig. 3(b) shows the equivalent circuit when $S2$ is conducting. The initial conditions are

$$i_L(0) = 0, \quad v_{c1}(0) = V_{12}, \quad v_{c2}(0) = V_{22}. \tag{4.1}$$

During this state the inductor current and the capacitor voltages are given by

$$i_L(t) = -\frac{V_{22}}{z_r}\sin\omega_r t \tag{4.2}$$

$$\begin{aligned} v_{c1}(t) &= (V_{in} - V_o - V_{12})(1 - \cos\omega_r t) + V_{12} \\ &= (V_{in} - V_o) - V_{22}\cos\omega_r t \end{aligned} \tag{4.3}$$

$$v_{c2}(t) = V_{22}\cos\omega_r t. \tag{4.4}$$

The input and output currents become

$$i_{in}(t) = i_o(t) = -\frac{1}{2}i_L(t) \quad \text{where} \quad 0 \le t \le \frac{T_r}{2}. \tag{4.5}$$

S3 conduction state Fig. 3(c) shows the equivalent circuit when $S3$ is conducting. The initial conditions are

$$i_L(0) = 0, \quad v_{c1}(0) = V_{13}, \quad v_{c2}(0) = V_{23}. \tag{5.1}$$

Again the inductor current and the capacitor voltages are

$$i_L(t) = -\frac{(V_{23} + V_o)}{z_r}\sin\omega_r t \tag{5.2}$$

$$\begin{aligned} v_{c1}(t) &= (V_{in} - V_{13})(1 - \cos\omega_r t) + V_{13} \\ &= V_{in} - (V_o + V_{23})\cos\omega_r t \end{aligned} \tag{5.3}$$

$$v_{c2}(t) = -V_o + (V_o + V_{23})\cos\omega_r t. \tag{5.4}$$

The input and output currents are

$$i_{in}(t) = -i_o(t) = -\frac{1}{2}i_L(t) \tag{5.5}$$

where

$$0 \le t \le \frac{T_r}{2}.$$

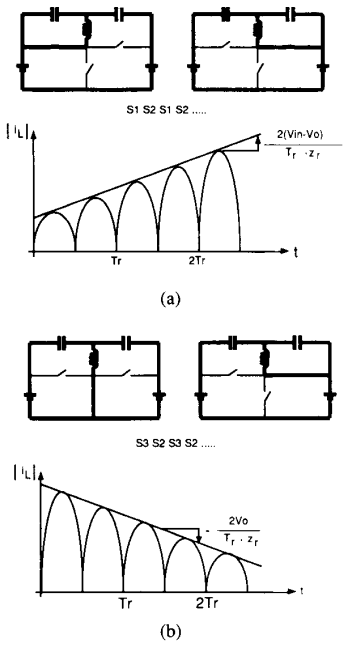

Fig. 4. Variation rate of the absolute peak inductor current. (a) Energizing mode. (b) De-energizing mode.

B. Operation Modes

The converter has two operating modes which are named as energizing mode and de-energizing mode.

Energizing mode: S1 and S2 are switched on and off alternatively at the instant of zero inductor current. During this mode, the amplitudes of v_{c1} and v_{c2} increase, that is, the source energy is delivered to the LC tank including the load. If $S1$ is turned on with $v_{c1}(0) = V_1 > 0$ and $v_{c2}(0) = -V_2 < 0$ at $t = 0$, then the magnitudes of the capacitor voltages at every zero crossing instant of the inductor current are given by

$$\begin{aligned} |v_{c1}(mT_r/2)| &= |v_{c1}[(m+1)T_r/2]| \\ &= V_1 + m(V_{in} - V_o) \end{aligned} \tag{6.1}$$

$$\begin{aligned} |v_{c2}(mT_r/2)| &= |v_{c2}[(m-1)T_r/2]| \\ &= V_2 + m(V_{in} - V_o) \\ &= V_1 + (m-1)(V_{in} - V_o) \end{aligned} \tag{6.2}$$

where

$$m = 2k, \quad k = 0, 1, 2, \ldots.$$

Equation (6.1), (6.2) and (6.3) show that the amplitudes of v_{c1} and v_{c2} increase by $2(V_{in} - V_o)$ for every resonant cycle of the energizing mode. From (3.2), (4.2), (6.1) and (6.2), the peak absolute value of the inductor current for the k_{th} half resonant period is given by

$$|i_{Lp}(k)| = \frac{V_1 + k(V_{in} - V_o)}{z_r}. \tag{6.3}$$

Equation (6.3) shows that the peak absolute value of i_L increases by $(V_{in} - V_o)/z_r$ for every half resonant period $T_r/2$ as shown in Fig. 4(a).

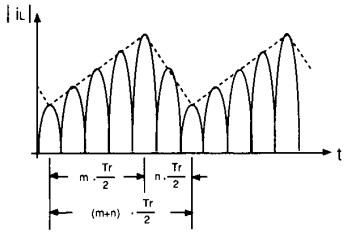

Fig. 5. The absolute inductor current waveform in steady state.

De-energizing mode: $S2$ and $S3$ are switched on and off alternatively at the instant of zero inductor current. In this mode, the LC tank energy is delivered to the source and the load. If $S3$ is turned on with $v_{c1}(0) = V_1 > 0$ and $v_{c2}(0) = -V_2 < 0$ at $t = 0$, then the magnitudes of the capacitor voltages at every zero crossing instant of the inductor current are given by

$$|v_{c1}(nT_r/2)| = V_1 - nV_o \tag{7.1}$$

$$|v_{c1}[(n+1)T_r/2]| = V_1 - 2V_{in} - nV_o \tag{7.2}$$

$$\begin{aligned} |v_{c2}(nT_r/2)| &= |v_{c2}[(m+1)T_r/2]| \\ &= V_2 - nV_o \end{aligned} \tag{7.3}$$

where

$$n = 2k, \quad k = 0, 1, 2, \ldots.$$

From (4.2), (5.2), (7.1), (7.2) and (7.3), the peak absolute value of the inductor current for the k_{th} half resonant period is given by

$$|i_{Lp}(k)| = \frac{V_2 - (k+1)V_o}{z_r}. \tag{7.4}$$

Equation (7.4) shows that the peak absolute value of i_L decreases by V_o/z_r for every half resonant period as shown in Fig. 4(b). In the steady state, the increment of $|i_{Lp}|$ during the energizing interval and the decrement of $|i_{Lp}|$ during the de-energizing interval becomes equal as shown in Fig. 5. Thus we can write

$$\frac{(V_{in} - V_o)}{z_r} \cdot m = \frac{V_o}{z_r} \cdot n \tag{8}$$

where m is the number of the energizing half cycle and n is the number of the de-energizing half cycle. Therefore the voltage conversion ratio M is given by

$$M = \frac{V_o}{V_{in}} = \frac{m}{m+n}. \tag{9}$$

This procedure of deriving M can be applied to any types of quantum converters.

C. Equivalent Circuit

From (9), we know that this converter is a buck type QSRC, thus it can be modeled as PWM buck converter as shown in

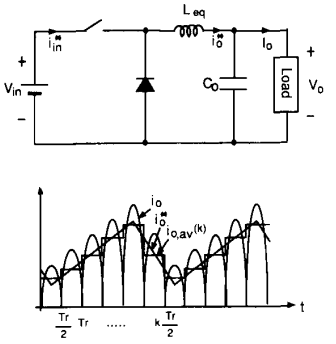

Fig. 6. The equivalent circuit and the current waveform.

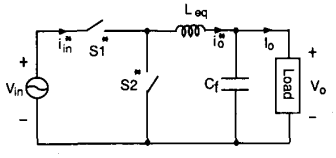

Fig. 7. The equivalent circuit of the ac chopper.

Fig. 6(a). Also as shown in Fig. 6(b), the stepped waveform of the average i_o for the k_{th} half resonant period, $i_{o,av}(k)$ can be converted into a continuous current i_o^* which is the equivalent current flowing through L_{eq}. In this case, $i_{o,av}(k)$ is given by

$$i_{o,av}(k) = \frac{2}{T_r}\int_{(k-1)\cdot T_r/2}^{k\cdot T_r/2} i_o(t)dt = \frac{1}{\pi}|i_{Lp}(k)|. \tag{10}$$

For the current i_o^* equivalent switching period, T_s^* becomes

$$T_s^* = (m+n)\frac{T_r}{2} \tag{11}$$

and the duty ratio D is given by

$$D = \frac{m}{m+n}. \tag{12}$$

Thus the equivalent inductance L_{eq} is given by

$$L_{eq} = \pi^2 L. \tag{13}$$

IV. Design Parameters of AC Chopper

Since the line frequency is quite lower than the switching frequency, the results of the previous chapter can be directly applied to the ac chopper shown in Fig. 1(a) which can operate, differently from dc case, at a inductive load. Fig. 7 shows the equivalent circuit where the equivalent switching period and the duty ratio are given by (12) and (13), respectively.

Fig. 8 shows the waveform of i_o^* whose peak value is given by

$$i_{o,p}^* = I_o + \frac{1}{2}\Delta I_o = I_o + \frac{m\cdot n}{m+n}\cdot\frac{V_{in}}{2\pi z_r}. \tag{14}$$

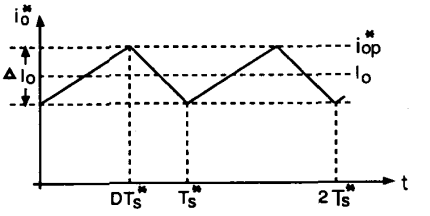

Fig. 8. The waveform i_o^*.

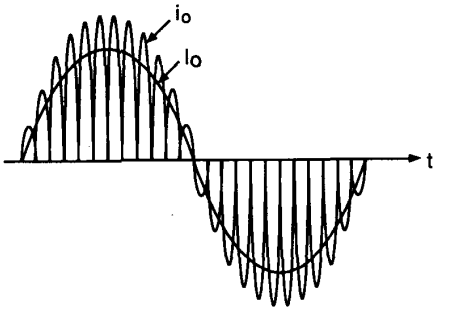

Fig. 9. Simplified waveform of i_o.

Since the magnitude of i_{Lp} is $2\cdot(\pi/2)\cdot i_o^*$, the maximum peak value of i_L becomes

$$i_{Lp,\max} = \pi I_{op,\max} + \frac{m\cdot n}{m+n}\cdot\frac{V_{in,p}}{2z_r} \tag{15}$$

where $I_{op,\max}$ is the peak value of the output current for full load and $V_{in,p}$ is the peak input voltage. Since the switch that is in conduction for the last half resonant period in the energizing mode is $S2$, from (4.3) and (4.4), we obtain

$$|v_{c1,p,\max}| = z_r i_{Lp,\max} + \frac{n}{m+n}V_{in,p} \tag{16}$$

$$|v_{c2,p,\max}| = z_r i_{Lp,\max} \tag{17}$$

where $v_{c1,p,\max}$ and $v_{c2,p,\max}$ are the peak capacitor voltages at the full load, respectively, for the peak input voltage, . In Fig. 8, the difference between the rms values of i_o^* and I_o is less than 4% of I_o if ΔI_o is less than I_o. So in calculating the rms current, the output current i_o can be considered as a simplified waveform as shown in Fig. 9. Thus the approximate rms value of i_L becomes

$$i_{L,rms} = 2i_{o,rms} \approx \frac{\pi}{\sqrt{2}}I_{o,rms}. \tag{18}$$

Since the equivalent conducting durations of $S1$, $S2$ and $S3$ for a given switching period are $(m/2)\cdot(T_r/2)$, $[(m+n)/2]\cdot(T_r/2)$ and $(n/2)\cdot(T_r/2)$, respectively, the rms currents of the switches are obtained by

$$i_{s1,rms} \approx \frac{\pi}{2}I_{o,rms}\sqrt{\frac{m}{m+n}} \tag{19}$$

$$i_{s2,rms} \approx \frac{\pi}{2}I_{o,rms} \tag{20}$$

$$i_{s3,rms} \approx \frac{\pi}{2}I_{o,rms}\sqrt{\frac{n}{m+n}}. \tag{21}$$

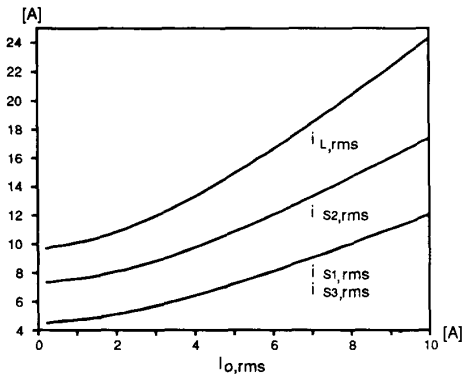

Fig. 10. The rms currents with variation of the output current V_in= 220 V_{rms}, V_o= 110 V_{rms}, line frequency = 60 Hz, z_r= 14 Ω, D= 0.5, maximum ΔI_o= 7.

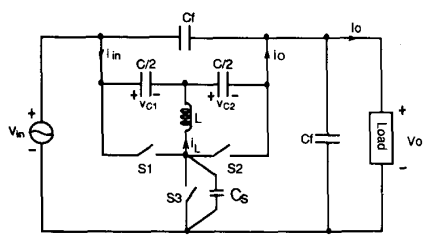

Fig. 11. ZVS ac/ac QSRC.

Fig. 10 shows the rms currents of the inductor and switches versus the output current. Above 5 A of $I_{o,rms}$, the simulation results coincide with the equations for the device rms currents. Below 5 A of $I_{o,rms}$, however, the simulation results are different from the equations because ΔI_o is larger than I_o in this range. The current flows more through $S2$ than the other switches because $S2$ conducts in both energizing and de-energizing modes. Maximum voltage stresses of the switches are given by

$$v_{s1,\max} = v_{s3,\max} = V_{in.p} \tag{22}$$

$$v_{s2,\max} = \frac{m}{m+n} V_{in,p} \quad \text{or} \quad \frac{n}{m+n} V_{in,p}. \tag{23}$$

The switches of the ac chopper shown in Fig. 1(a), are turned on and off at each zero current instant. On the other hand, Fig. 11 shows a zero-voltage-switching QSRC. C_s is a soft commutation capacitor of the switches. The conducting switch is turned off before the inductor current decays to zero and then the next switch is turned on when zero voltage switching condition is met. The switching frequency is slightly higher than that of ZCS QSRC but all of the design equations for the ZCS ac/ac QSRC can be applied to this converter. This converter has more novel switching condition but slightly narrower load range than the ZCS ac/ac QSRC.

V. Experimental Results

In the experiment, the ZCS ac/ac QSRC shown in Fig. 6 is used. The converter is designed to have $220V_{rms}$ of the input voltage, 60 Hz of the line frequency and 1 kVA of the maximum output power at 100 kHz of the switching frequency. The circuit parameters are given as follows:

$$L = 22\mu H$$
$$C_1 = C_2 = 47nF$$
$$C_f = 47\mu F$$
$$z_r = 14\Omega$$
$$f_r = 100 \text{ kHz}$$

The control duty is chosen to 0.5 by selecting

$$m = 2 \text{ and } n = 2.$$

The input and output voltage waveforms are shown in Fig. 12. The output voltage is slightly lower than the half input voltage because of the conduction voltage drops of the switches. Fig. 13 shows v_{c1} and i_L at $I_{o,rms} = 10A$. At full load, the measured efficiency was 86%. At resistive load, the output voltage and the inductor current is in phase as shown in Fig. 14. For the inductive load, however, the inductor current is delayed as shown in Fig. 15. It also shows that this ac chopper has the capability of 4 quadrant operation.

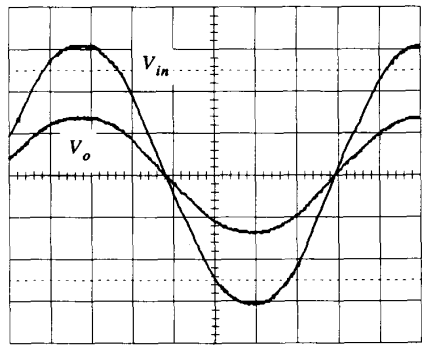

Fig. 12. The input and output voltage waveforms 100 V/div, 2 ms/div.

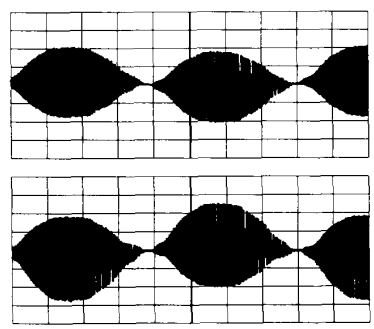

Fig. 13. The capacitor voltage (v_{c1}) and inductor current waveforms at a full load (I_o = 10). Upper trace: v_{c1}(500 V/div). Lower trace: i_L (20 A/div). Time: 2 ms/div.

VI. Conclusion

A new ZCS QSRC is proposed and applied to the pure sinewave 60 Hz ac chopper (220/110 V electronic step down transformer) which has the capability of 4 quadrant operation.

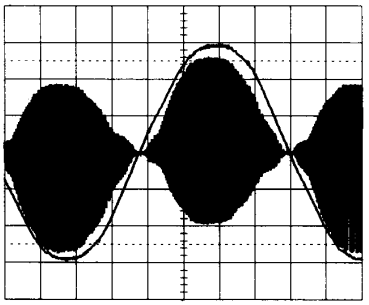

Fig. 14. The output voltage and inductor current waveforms at a resistive load. Outer trace: ν_o (50 V/div). Inner trace: i_L (20 A/div). Time: 2 ms/div.

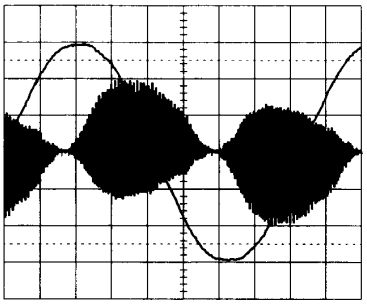

Fig. 15. The output voltage and inductor current waveforms at an inductive load. Outer trace: ν_o (50 V/div). Inner trace: i_L (20 A/div). Time: 2 ms/div.

For a fixed switching pattern, the ac chopper has constant voltage conversion ratio regardless of the magnitude and polarity of the input voltage. The voltage ratio is also independent of the load variation. The analytical method of deriving the conversion ratio of the quantum converter is shown and the design equations are derived. The characteristic of the very low no load loss compensates the shortcoming of somewhat low full load efficiency. In the power rating below a few kVA, the proposed ac chopper can replace the iron cored step down transformer for home appliances which has low operation duty. AC chopper is thought to be convenient in use because of its small size and weight if the complicated controller is replaced by a one chip ASIC. The operation of the ac chopper is verified by the experiment.

ACKNOWLEDGMENT

The authors appreciate the contribution of S. E. Park, Y. Suk Kang, and Tae Sung Kim of Applied Electronic Department, Research Center, KEPCO.

REFERENCES

[1] K. H. Liu, R. Oruganti and F. C. Y. Lee, "*Quasi-Resonant Converters - Topologies and Characteristics*", IEEE Trans. on PE-2, No. 1, pp. 62–71, Jan. 1987.

[2] W. A. Tabisz and F. C. Lee, "*Zero-Voltage-Switching Multi-Resonant Technique - A Novel Approach to Improve Performance of High-Frequency Quasi-Resonant Converters*", IEEE PESC Rec. pp. 9–17, 1988.

[3] D. M. Divan, "*Pseudo-Resonant Full Bridge DC/DC Converter*", IEEE PESC Rec., pp. 424–430, 1988.

[4] I. D. Kim, E. C. Nho and G. H. Cho, "*A Soft Switching Constant Frequency PWM DC/DC Converter with Low Switch Stress and Wide Linearity*", Proceeding of 16th Annual Conference of IEEE Industrial Electronics Society pp. 875–881, 1990.

[5] F. C. Schwarz, "*An Improved Method of Resonant Current Pulse Modulation for Power Converters*", IEEE Trans. Industrial Electronics and Control Instruments, Vol. IECI-23 No. 2, pp. 133–141, May 1976.

[6] G. B. Joung, C. T. Rim and G. H. Cho, "*An Integral Cycle Mode Control of Series Resonant Converter*", IEEE PESC Rec., pp. 575–582, 1988.

[7] G. B. Joung, C. T. Rim and G. H. Cho, "*Modeling of Quantum Series Resonant Converters - Controlled by Integral Cycle Mode*", IEEE Industry Application Society Annual Meeting, pp. 821–826, 1988.

[8] G. B. Joung, J. G. Cho and G. H. Cho, "*Generalized Quantum Resonant Converters Using A New Concepts of Quantum Resonant Switch*", IEEE PESC Rec., pp. 847–854, 1990.

[9] R. J. King and T. A. Stuart, "*A Large-Signal Dynamic Simulation for The Series Resonant Converter*", IEEE AES Vol. AES-19, No. 6, pp. 859–870, Nov. 1983.

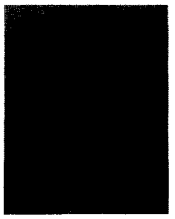

Dong Y. Huh was born in Korea in 1961. He received the B.S. degree in electronics engineering from Kyung Pook National University, Taegu, Korea, and the M.S. degree in electrical and electronics engingeering from the Korea Advanced Institute of Science and Technology (KAIST), Seoul, in 1987 and 1989, respectively.

He is presently working toward the Ph.D. degree at KAIST. His research interests are design of resonant converters, high-frequency power converters and SMPS, and design and control of electronic ballasts.

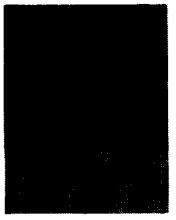

Gyu H. Cho was born in Korea on April 19, 1953. He received the M.S. and Ph.D. degrees from KAIST in 1977 and 1981, respectively.

During 1982–1983, he was with the Electronic Technology Division of Westinghouse R&D Center, Pittsburgh, PA, where he worked on unrestricted frequency changer systems and inverters. In 1989, he was a visiting professor of University of Wisconsin, Madison. Since 1984, he has been an Assistant/Associate Professor with the Electrical and Electronics Department of KAIST, where he is currently a professor. His research interests are in the areas of static power converters, drivers and resonant converters, and recently, he has been interested in MOS and bipolar integrated circuit design.